Table V. $^{31}P\{^1H\}$ NMR Parameters for Cations $[Ag(PR_3)_2]^+$ (4) (Measured in CD_3COCD_3 at −80 °C)

complex	$\delta(^{31}P)$	$^1J(^{107}Ag,^{31}P^1)$, Hz	$^1J(^{109}Ag,^{31}P)$, Hz
4a	8.3	484	558
4b	43.9	468	540
4c	40.3	446	515
4d	10.7	492	530

compounds occur at lower fields than in the corresponding mononuclear platinum complexes. These low-field shifts are larger for the gold compounds (ca. 5 ppm) than for the silver complexes (ca. 2 ppm). It is noteworthy that these low-field shifts on bridge formation appear to be qualitatively related to the thermal stability of the bimetallic compounds, as the $\Delta\delta$ values of the related Pt/Hg complexes of the type $[(PEt_3)(C_6Cl_5)Pt(\mu\text{-}H)HgR]^+$, which decompose above −40 °C, are of the order of ca. 8 ppm.[18]

Corresponding changes are also observed in parameters such as $^1J(Pt,P^2)$ and $^2J(P,H)$ (see Table IV). While in the former case the changes of these parameters on bridge formation are more comparable in the gold and silver compounds ($\Delta J \simeq 450$ Hz), in the latter case the $\Delta J(Au)$ values are ca. 8 Hz and $\Delta J(Ag)$ values are ca. 3 Hz.

All the above data can be taken as an indication that the Au–H bond is likely to be stronger than the corresponding Ag–H bond.

In this context it is noteworthy that when complexes such as *trans*-$[PtH(C_6Cl_5)(PEt_3)_2]$ are reacted with species such as $Cu(P\text{-}i\text{-}Pr_3)^+$ cations, no interaction can be detected even at ca. −70 °C.

Finally, the values of the Pt,Ag-coupling constants in complexes **1b**, **1c**, and **1e** are of the order of 400 Hz. The relationship between these values and the degree of Pt–Ag interaction is unclear, particularly because very few Pt–Ag constants are known, e.g., those published by van der Ploeg et al.,[32] which, however, are for compounds of very different structures. Thus the $J(Pt,Ag)$ values in compounds of type **5** are of the order of ca. 170 Hz.

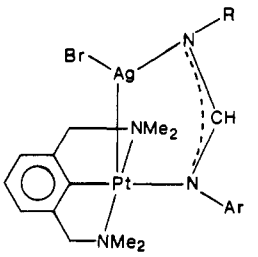

5

However, as can be seen from their structure, the Pt–Ag interactions are very different from those occurring in complexes containing Pt–H–Ag bridges.

As solutions of compounds of type **1** also contain the cations $[Ag(PR_3)_2]^+$ (**4**), their ^{31}P NMR parameters are listed in Table V. The values of the $^1J(Ag,P)$ coupling constants are of the order of magnitude expected for two-coordinate silver.[33]

Acknowledgment. H.L. and M.W. received support from the Swiss National Science Foundation, and A.A. acknowledges financial support from the Italian MPI. We are greatly indebted to Dr. P. S. Pregosin for valuable discussion and S. Chaloupka for experimental assistance.

Supplementary Material Available: Figure S1, showing the numbering scheme, and Tables S1 and S2, giving final positional and thermal parameters and an extended list of bond lengths and angles (5 pages); Table S3, listing observed and calculated structure factors (16 pages). Ordering information is given on any current masthead page.

(32) Van der Ploeg, D. F. M. J.; van Koten, G.; Brevard, C. *Inorg. Chem.* **1982**, *21*, 2878.

(33) Camalli, M.; Caruso, F.; Chaloupka, S.; Kapoor, P. N.; Pregosin, P. S.; Venanzi, L. M. *Helv. Chim. Acta* **1984**, *67*, 1603 and references quoted therein.

Contribution from the Departments of Chemistry and Physics, Syracuse University, Syracuse, New York 13244-1200

Gas-Phase One-Photon Electronic Spectroscopy of (Arene)chromium Tricarbonyls: Substituent Effects in Multiphoton Dissociation/Ionization Spectra

Dan Rooney,† J. Chaiken,*† and D. Driscoll‡

Received January 15, 1987

We have measured the first gas-phase electronic absorption spectra of $(\eta^6\text{-}C_6H_6)Cr(CO)_3$, $(\eta^6\text{-}C_6H_5Cl)Cr(CO)_3$, and $(\eta^6\text{-}C_6H_5CH_3)Cr(CO)_3$. Low-resolution, 200-$cm^{-1}$, spectra show intense (92 000 L/(mol cm)) absorption features extending into the vacuum ultraviolet region indicating the existence of at least five different electronic states with energies below 61 000 cm^{-1}. Our low-resolution data suggest that only one of those states shifts appreciably with arene substitution. We compare these results with solution-phase spectra and other data. At higher resolution, 40 cm^{-1}, our data suggest that the onset of detectable absorption is lower in energy for $(\eta^6\text{-}C_6H_6)Cr(CO)_3$ than for both $(\eta^6\text{-}C_6H_5Cl)Cr(CO)_3$ and $(\eta^6\text{-}C_6H_5CH_3)Cr(CO)_3$. The fine structure of this transition may be correlated with the well-known photolability of the CO ligands. We discuss these new data in the light of our earlier multiphoton spectroscopy results on these molecules.

Introduction

There are relatively few gas-phase one-photon UV–visible absorption spectra available for organometallic molecules, especially those with non-carbonyl ligands, yet such spectra provide valuable information concerning electronic structure and bonding. The nature of the η^6 Cr–arene bond in $(\eta^6\text{-arene})Cr(CO)_3$ complexes and the effects of coordination on the electronic structure[1-3] and reactivity patterns[4,5] of the arene ligand are questions of

† Department of Chemistry.
‡ Department of Physics.

(1) Eisenstein, O.; Hoffmann, R. *J. Am. Chem. Soc.* **1981**, *103*, 4308 and references therein.
(2) Elian, M.; Chen, M. M. L.; Mingos, D. M. P.; Hoffmann, R. *Inorg. Chem.* **1976**, *15*, 1148.
(3) Albright, T. A.; Hofmann, P.; Hoffmann, R. *J. Am. Chem. Soc.* **1977**, *99*, 7546.

0020-1669/87/1326-3939$01.50/0 © 1987 American Chemical Society

considerable fundamental and practical importance. Previously[6-8] we have employed one-color UV–visible multiphoton dissociation/ionization spectroscopy (MPD/MPI) to probe the higher electronic states of (arene)chromium tricarbonyls (ACTs). We wish to compile as complete a listing of the energies and symmetry types of the electronic states of the ACTs as possible. We are searching for excited electronic states of organometallic molecules in which specific ligand to metal bonds can be selectively broken. We obtained these one-photon absorption spectra to complement our multiphoton spectra.

One reason for choosing to study ACTs is that they are quite well characterized experimentally and so much background information[9] is available for correlation with our data. We also choose (arene)chromium tricarbonyl systems for study because of the expected differences between the metal to CO bonding and the η^6 metal to arene bonding. The one-photon-induced chemistry of ACTs is known[10,11] to be dominated by initial loss of CO via absorption of a single photon of 55000-cm^{-1} energy or less. Unlike the case of CO ligands, photodissociation of an arene ligand from a metal center may involve η^4- or η^2-bonded intermediates. The thermal chemistry of ACTs[4,5,9] almost always involves dissociation or modification of the arene ligand. If we managed to find a means for photoexciting ACTs that involved loss of arene, we might suspect that we had discovered a new photochemical pathway for these molecules. Whether this pathway involves selective loss of arene would then have to be independently determined. Initially, we would be satisfied to demonstrate that such pathways might exist and that it is possible to induce molecules to follow these paths. This is a long-range goal of our research.

Unavoidably, we require knowledge of the radiationless dynamics of these molecules. Our interpretation of the MPD/MPI results[6-8] suggests that the competition between the rate of radiationless transitions associated with intramolecular vibrational relaxation, photodissociation, and the rate of multiphoton excitation determines the branching ratio between certain pathways of MPD/MPI. The question of whether the rate of CO photolabilization occurs quickly enough on the lowest energy excited electronic potential surface to influence the course of MPD/MPI is central to our interpretation. The existence of excited electronic state(s) of appropriate energy and symmetry that would facilitate multiphoton absorption of a single wavelength will be demonstrated.

We present one-photon absorption spectra of representative ACTs that span from the onset of electronic absorption to the ionization potential in the vacuum ultraviolet region. Low-resolution scans are used to list those states that have energies below 61000 cm^{-1} and have gas-phase extinction coefficients of at least 1000 L/(mol cm). Possible splittings and shifts in these states, induced by arene substituents, are discussed in terms of previous solution-phase spectra and available calculations. A conclusion of this study is that better calculations utilizing modern methodologies are needed. Special attention is paid to the spectral region near the low-energy onset of absorption since the lowest energy states often dominate the photochemistry of molecules. Our highest resolution spectra reveal extensive fine structure that may be analogous to similar structure observed[12] in the absorption spectrum of $Cr(CO)_6$. Solely on the basis of the observability of this structure, we provide a lower limit on the nonradiative decay lifetime of the upper states in the transitions.

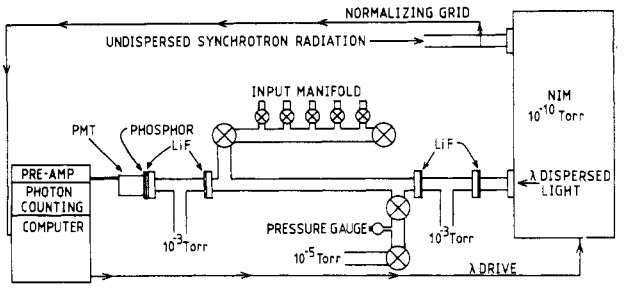

Figure 1. Apparatus for measuring absorption spectra.

Experimental Section

The experimental apparatus is illustrated in Figure 1. The chemical and other gases were introduced through an isolated input manifold. The undispersed synchrotron radiation entered the absorption tube after first traversing a normalizing grid, a 1-m McPherson normal-incidence monochromator (NIM), and an isolation T-section fitted with LiF windows. The absorption cell windows and walls were heated to 145 ± 20 °C to maintain sufficient number density of the ACT in the light path. Room-temperature vapor pressures of these compounds are all less than 0.1 mTorr. The evacuated T-sections, 10^{-3} Torr, at either end of the absorption tube allow uniform baking while thermally isolating the photomultiplier (PMT), the sodium salicylate phosphor, and the monochromator. Absorption cell pressure measurements were made by using a thermocouple gauge. The accuracy of the pressure measurements was severely limited by the fact that the organometallics poison the thermocouple. For this reason we exposed the thermocouple only when necessary. The apparent recovery of the gauge response to an appropriate response to high vacuum between ACT exposures indicated the degree to which it was poisoned. Although absolute pressure readings could only be accurate to ±25%, relative readings are accurate to ±10%.

A typical experiment entailed measuring a background power spectrum with an evacuated static cell at total pressures of about 10^{-5} Torr. Another power spectrum obtained immediately thereafter combined with the background spectrum to obtain an absorption spectrum of the "empty" cell. Any chemical or other species that had been adsorbed onto the cell walls or windows and sublimed between the time the background and empty cell spectra were measured can then be detected by its absorption. Successive empty-cell absorption spectra were obtained until they were reproducibly flat and gave nearly an average absorption of zero across the scan range. The cell was usually flushed with argon a few times to accelerate the process. When the cell was clean, the valve isolating the input manifold was opened and the contents flowed into the absorption path. The input manifold and attached chemical reservoir were maintained about 10 °C cooler than the absorption tube. Chemical pressures of a few tens of a millitorr were obtained in the absorption tube in this fashion. A power spectrum of the chemical-filled tube was obtained, and with the most recent background power spectrum used as background, an absorption spectrum of the gas-phase chemical was calculated. The absorbances in the displayed low-resolution spectra were corrected for the measured pressure of the ACTs and the absorption path length. Because of the above-mentioned problem concerning pressure measurements, the absolute accuracy of the extinction coefficients so obtained does not exceed ±25%. We have attempted to be quantitative because we know of very few published values of gas-phase extinction coefficients for organometallic molecules.

Radiation wavelength was scanned in 20-, 10-, 5-, and 2.5-Å steps in either direction with 16.7-, 10-, 5-, and 1.6-Å bandwidths, respectively. The scans displayed here are presented as linear in energy so the bandwidth and hence resolution vary across a spectrum. For the data we present, the high-resolution scans have a resolution of 14 cm^{-1} near the long-wavelength limit and 44 cm^{-1} near the short-wavelength limit. The low-resolution spectra correspond to 49- and 350-cm^{-1} resolution near the long- and short-wave length limits, respectively.

The light was detected by using a water-cooled photomultiplier whose response was extended into the VUV region by means of a sodium salicylate phosphor. Light intensity was measured by photon counting. The light intensity was proportional to the number of PMT counts obtained in the time required to obtain 5 × 10^5 photon counts from the normal-

(4) Pearson, A. J. *Science (Washington, D.C.)* **1984**, *223*, 895.
(5) Jaouen, G. In *Transition Metal Organometallics in Organic Synthesis*; Alper, H.; Ed.; Academic: New York, 1978; Vol. 2, pp 65–120. Semmelhack, M. F. *Tetrahedron* **1981**, *37*, 3956; *Ann. N.Y. Acad. Sci.* **1977**, *295*, 36.
(6) Hossenlopp, J. M.; Rooney, D.; Samoriski, B.; Chaiken, J. *Chem. Phys. Lett.* **1985**, *116*, 380.
(7) Samoriski, B.; Hossenlopp, J. M.; Rooney, D.; Chaiken, J. *J. Chem. Phys.* **1986**, *86*, 3326.
(8) Hossenlopp, J. M.; Samoriski, B.; Rooney, D.; Chaiken, J. *J. Chem. Phys.* **1986**, *86*, 3331.
(9) *Comprehensive Organometallic Chemistry*; Wilkinson, G., Ed.; Pergamon: Oxford, 1982; Vol. 3, p 1021.
(10) Wrighton, M. S.; Haverty, J. L. *Z. Naturforsch., B: Anorg. Chem., Org. Chem.* **1975**, *30B*, 254.
(11) Geoffroy, G.; Wrighton, M. S. *Organometallic Photochemistry*; Academic: New York, 1979. Gilbert, A.; Kelly, J. M.; Budzwait, M.; Koerner Von Gustorf, E. *Z. Naturforsch.*, **1976**, *31B*, 1091.
(12) Trogler, W. C.; Desjardins, S. R.; Solomon, E. I. *Inorg. Chem.* **1979**, *18*, 2131–2136.

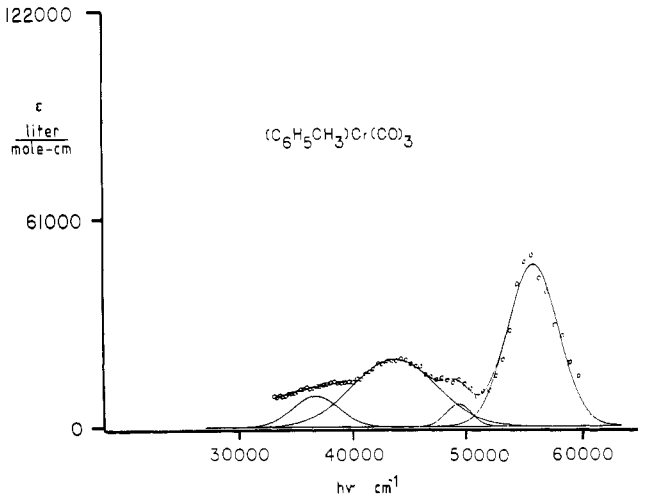

Figure 2. Low-resolution absorption spectrum of $(\eta^6\text{-}C_6H_5CH_3)Cr(CO)_3$. Data points are open circles. Predicted spectrum and composite Gaussians are as indicated.

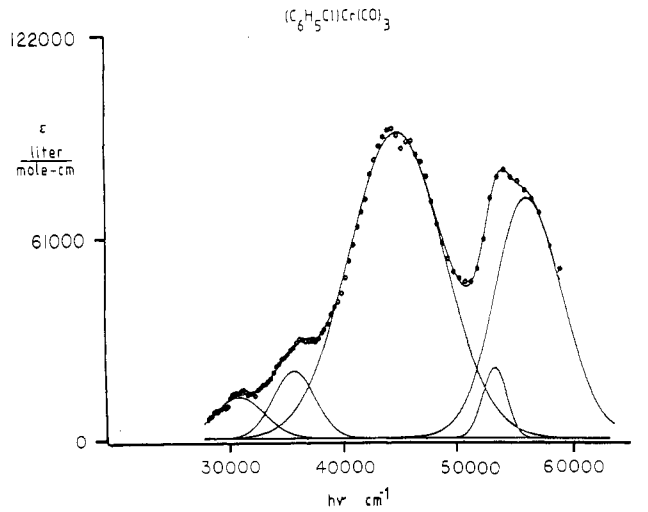

Figure 3. Low-resolution absorption spectrum of $(\eta^6\text{-}C_6H_5Cl)Cr(CO)_3$. Data points are open circles. Predicted spectrum and composite Gaussians are as indicated.

izing grid. The normalizing grid is a highly transparent tungsten mesh that, by the photoelectric effect, provides a photocurrent proportional to the synchrotron radiation intensity integrated over energies above the tungsten work function. Such an arrangement allows for automatic compensation for the drift in synchrotron beam current. The signal to noise ratio was roughly 100:1. Photomultiplier power supply voltage settings were based on measured response curves, and count rates were kept below the point where sampling errors due to coincidence effects occurred.

Chemicals were prepared by a standard procedure[8,13] and purified by sublimation. NMR, IR, and melting point analyses were performed on the samples before *and after* the experiments to check for thermal stability and purity. The chemical-reservoir and absorption-cell temperatures were kept well below the thermal decomposition points of the compounds. GLC mass spectrometric studies[14] at column temperatures ranging from 120 to 180 °C indicated that no decomposition occurs. Additional evidence[15] for thermal stability comes from a separate gas chromatographic study where UV–visible spectra of ACTs eluted from columns held at temperatures up to 200 °C indicated that no decomposition occurs. Other workers[16] indicate that the ACT compounds are stable up to 300 °C. Spectra were obtained in flowing and static cell arrangements in our system, which also indicated no significant decomposition occurs either thermally or photochemically.

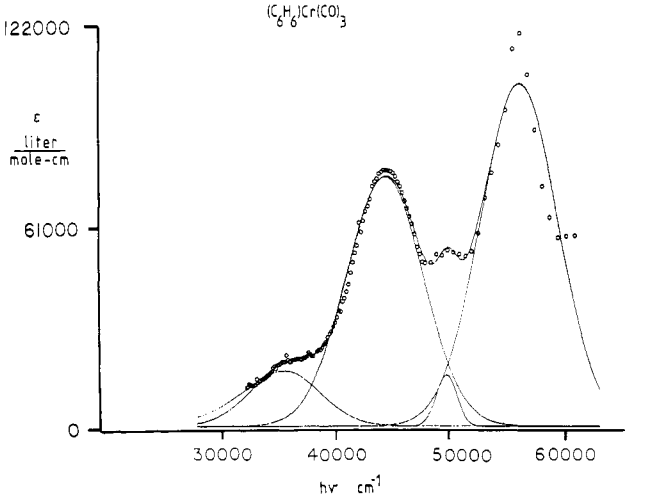

Figure 4. Low-resolution absorption spectrum of $(\eta^6\text{-}C_6H_6)Cr(CO)_3$. Data points are open circles. Predicted spectrum and composite Gaussians are as indicated.

Table I. Absorption Spectral Data for $(\eta^6\text{-}C_6H_5Cl)Cr(CO)_3$

observed			Gaussian fit analysis[a]			
ln (I_0/I)	ϵ_{max}, L·mol^{-1}·cm^{-1}	ν_{max}, cm^{-1}	ln (I_0/I)	ϵ_{max}, L·mol^{-1}·cm^{-1}	$\theta_{1/2}$, cm^{-1}	ν_{max}, cm^{-1}
3.08	76 000	55 600	3.08	72 000	4590	55 500
3.30	81 000	53 800	3.31	22 000	1400	52 800
3.77	92 000	44 300	3.76	92 000	5600	44 400
1.25	31 000	36 200	1.24	23 000	2550	35 800
0.624	15 000	31 400	0.56	13 000	3000	31 100

[a] The Gaussians are of the form $\ln (I_0/I) = \epsilon_{max} e^{-(\nu-\nu_{max})^2\theta_{1/2}^2}$, where ϵ_{max} is the peak absorbance of a feature, ν_{max} is the center frequency, and $\theta_{1/2}$ is the half-width at half-height.

Table II. Absorption Spectral Data for $(\eta^6\text{-}C_6H_5CH_3)Cr(CO)_3$

observed			Gaussian fit analysis			
ln (I_0/I)	ϵ_{max}, L·mol^{-1}·cm^{-1}	ν_{max}, cm^{-1}	ln (I_0/I)	ϵ_{max}, L·mol^{-1}·cm^{-1}	$\theta_{1/2}$, cm^{-1}	ν_{max}, cm^{-1}
2.24	56 000	54 900	2.13	48 000	2900	55 100
0.57	14 000	49 000	0.56	7000	1500	49 000
0.84	21 000	44 200	0.83	19 000	4900	43 800
0.43	12 000	35 500	0.44	9600	2700	37 200
0.30	7300	30 400				

Table III. Absorption Spectral Data for $(\eta^6\text{-}C_6H_6)Cr(CO)_3$

observed			Gaussian fit analysis			
ln (I_0/I)	ϵ_{max}, L·mol^{-1}·cm^{-1}	ν_{max}, cm^{-1}	ln (I_0/I)	ϵ_{max}, L·mol^{-1}·cm^{-1}	$\theta_{1/2}$, cm^{-1}	ν_{max}, cm^{-1}
3.33	81 000	55 500	2.96	72 000	4600	56 000
1.54	38 000	49 500	1.56	11 000	1200	49 500
2.23	55 000	44 200	2.23	53 200	4600	44 300
0.63	15 000	35 800	0.57	13 000	4300	35 800
0.27	6600	28 300				

Results

Low-resolution absorption spectra of $(\eta^6\text{-}C_6H_5CH_3)Cr(CO)_3$, $(\eta^6\text{-}C_6H_5Cl)Cr(CO)_3$, and $(\eta^6\text{-}C_6H_6)Cr(CO)_3$ are displayed in Figures 2–4. Higher resolution spectra of all three molecules are displayed in Figure 5. These spectra correspond to about 10-mTorr ACT pressure. A spectrum of $Cr(CO)_6$ was obtained that closely resembled the published work of Russell.[17] The observed absorption maxima are summarized, along with other pertinent results, in Tables I–III.

(13) Nicholls, B.; Whiting, M. C. *J. Chem. Soc.* **1959**, 551.
(14) Van Den Heuvel, W. J. A.; Keller, J. S.; Veening, H.; Willeford, B. R. *Anal. Lett.* **1970**, *3*, 279.
(15) Veening, H.; Graver, N. J.; Clark, D. B.; Willeford, B. R. *Anal. Chem.* **1969**, *41*, 1655.
(16) Gilbert, J. R.; Leach, W. P.; Miller, J. R. *J. Organomet. Chem.* **1973**, *49*, 219.
(17) Iverson, A.; Russell, B. R. *Chem. Phys. Lett.* **1970**, *6*, 307.

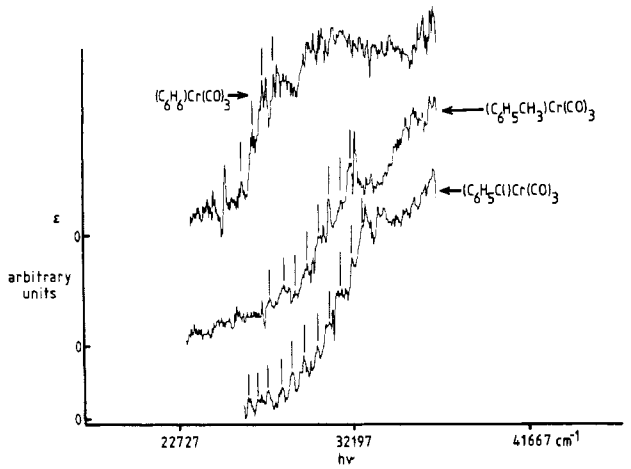

Figure 5. High-resolution absorption spectra of ACTs near low-energy onset of absorption. Vertical lines designate members of a possible vibrational progression.

The low-resolution spectra of all the ACTs studied have absorption maxima within ±400 cm^{-1} of 36 300, 44 250, and 55 300 cm^{-1}. Our spectrum of $Cr(CO)_6$ has absorption maxima near 36 300 and 44 250 cm^{-1}. The 55 300-cm^{-1} feature is completely missing in the $Cr(CO)_6$ spectrum. Relative to the other features in the spectrum of the same molecule, the intensity of the 44 250-cm^{-1} feature decreases in the order (η^6-C_6H_5Cl)$Cr(CO)_3$ > $Cr(CO)_6$ > (η^6-C_6H_6)$Cr(CO)_3$ > (η^6-$C_6H_5CH_3$)$Cr(CO)_3$. Within the resolution of our experiment, we observed no shifts in the energy of the lower two bands as the arene substituent is varied.

At low resolution there are undulations near the maximum of the 44 250-cm^{-1} feature in the (η^6-C_6H_5Cl)$Cr(CO)_3$ spectrum, which do not appear in the (η^6-C_6H_6)$Cr(CO)_3$ spectrum. This feature is also broader in the (η^6-$C_6H_5CH_3$)$Cr(CO)_3$ spectrum than in that of (η^6-C_6H_6)$Cr(CO)_3$. In addition, the 55 300-cm^{-1} feature is broader in the (η^6-C_6H_5Cl)$Cr(CO)_3$ spectrum and shows a pronounced asymmetry, which is not present in the low-resolution (η^6-C_6H_6)$Cr(CO)_3$ or (η^6-$C_6H_5CH_3$)$Cr(CO)_3$ spectrum. The (η^6-C_6H_6)$Cr(CO)_3$ spectrum has a feature near 49 500 cm^{-1} that is not visible in the (η^6-C_6H_5Cl)$Cr(CO)_3$ spectrum but can be observed in the (η^6-$C_6H_5CH_3$)$Cr(CO)_3$ spectrum at nearly the same energy. We can state that there are at least five transitions clearly visible in our low-resolution scans and that there may be other transitions that are not as clearly visible in all the low-resolution spectra.

In an effort to clarify the shifts and splittings that may occur upon introducing the arene substituent by an unbiased procedure,[18-20] we attempted to decompose the spectra into sums of Gaussian peaks. The parameters obtained are given in the tables. All the (η^6-C_6H_6)$Cr(CO)_3$ and (η^6-$C_6H_5CH_3$)$Cr(CO)_3$ features above 31 000 cm^{-1} could be represented as a sum of at least four Gaussians. All the (η^6-C_6H_5Cl)$Cr(CO)_3$ features could be represented by five Gaussians. The lowest energy feature of (η^6-C_6H_6)$Cr(CO)_3$ or (η^6-$C_6H_5CH_3$)$Cr(CO)_3$ could not be fit by a single Gaussian. Attempts were made to fit all the observed features with other peak shape forms, e.g. Lorentzians, weighted Gaussians, etc., and these fits generally gave poorer sums of squares of residuals, never converged, or gave a statistically insignificant reduction in the sum of squares of residuals. The only exception was the feature near 55 300 cm^{-1} in the (η^6-C_6H_6)$Cr(CO)_3$ and (η^6-$C_6H_5CH_3$)$Cr(CO)_3$ spectra, which was better represented by a Lorentzian than a single Gaussian. Given that these features are inhomogeneously broadened and that our resolution near 55 300 cm^{-1} was about 400 cm^{-1}, we do not judge the exact shape of that particular feature to be well determined experimentally. The Gaussians alone could fit all the data to within 5% mean-square error, which was considered sufficient for the present analysis.

We made numerous attempts to represent the 44 250-cm^{-1} feature in the (η^6-C_6H_5Cl)$Cr(CO)_3$ spectrum as the sum of two Gaussians with no improvement in the sum of squares of residuals. The undulations would therefore seem to be more likely associated with vibronic structure although this Gaussian analysis is by no means unequivocal. In contrast, the 55 300-cm^{-1} feature in the (η^6-C_6H_5Cl)$Cr(CO)_3$ spectrum was properly fit by two Gaussians and the 55 300-cm^{-1} feature in the (η^6-C_6H_6)$Cr(CO)_3$ and (η^6-$C_6H_5CH_3$)$Cr(CO)_3$ spectra was reasonably well represented by only one Gaussian. The two Gaussians, which together fit the 55 300-cm^{-1} feature in the (η^6-C_6H_5Cl)$Cr(CO)_3$ spectrum, have vastly unequal widths. The 49 500-cm^{-1} feature in the (η^6-C_6H_6)$Cr(CO)_3$ and (η^6-$C_6H_5CH_3$)$Cr(CO)_3$ spectra is narrow compared to most other features. The 55 300-cm^{-1} feature in the (η^6-C_6H_6)$Cr(CO)_3$ and (η^6-$C_6H_5CH_3$)$Cr(CO)_3$ spectra is broad compared to most other features.

Starting at high energy, there is a correspondence between all the peaks of the ACTs that is suggested by the widths of the composite Gaussians. In each case the alternation of the widths is comparable for each molecule. According to this correspondence, only the feature that appears near 49 500 cm^{-1} in both the (η^6-C_6H_6)$Cr(CO)_3$ and (η^6-$C_6H_5CH_3$)$Cr(CO)_3$ spectra and near 52 800 cm^{-1} in the (η^6-C_6H_5Cl)$Cr(CO)_3$ spectrum shows any detectable shift in energy that correlates with the presence of the arene substituent. We stress that these are low-resolution data and other shifts and splittings may occur that are too small to observe at this resolution. However, if the Gaussian analysis has any validity, then it would appear that the one transition mentioned shifts roughly 3300 cm^{-1} to higher energy with monochlorination of the arene. While this shift is large enough to observe, the Gaussian analysis also indicates that methylation of the arene causes the same band to shift to lower energy by an amount that is only on the order of our spectral resolution. We are uncertain as to whether this shift is real and are planning to obtain more spectra at higher resolution in order to clarify the situation further. Since we were unable to fit the lowest energy features for the (η^6-C_6H_6)$Cr(CO)_3$ and (η^6-$C_6H_5CH_3$)$Cr(CO)_3$ low-resolution spectra, the above remarks do not apply to those features.

There is a band maximum near 30 400 cm^{-1} that is clearly visible at low-resolution in the (η^6-C_6H_5Cl)$Cr(CO)_3$ spectrum and appears only as an inflection on the low-energy side of the 36 300-cm^{-1} feature in the low-resolution (η^6-C_6H_6)$Cr(CO)_3$ spectrum. This feature is stronger and, at low resolution, would seem to appear at lower energy in the (η^6-C_6H_5Cl)$Cr(CO)_3$ spectrum compared to the (η^6-C_6H_6)$Cr(CO)_3$ low-resolution spectrum. The feature is even weaker in the (η^6-$C_6H_5CH_3$)$Cr(CO)_3$ spectrum.

The lowest energy spectral region was of particular interest to us so we recorded high-resolution scans specifically to try to find the onset of absorption. The extinction coefficients are small and quite different for each molecule, so when viewing Figure 4, one must bear in mind that the vertical scales for the different spectra are different. Because of our problems with pressure measurement, absolute absorption scales are not indicated. Our best estimate of the position of zero absorption, which was obtained by repeated measurements of empty-cell spectra, can be seen indicated in Figure 5. Visual characterization of the high-resolution spectra reveals that the (η^6-C_6H_6)$Cr(CO)_3$ spectrum has sparser and more abrupt vibrational structure. The growth in absorption strength is not nearly as steep in the (η^6-C_6H_5Cl)$Cr(CO)_3$ and (η^6-$C_6H_5CH_3$)$Cr(CO)_3$ spectra. The relative smoothness of the (η^6-$C_6H_5CH_3$)$Cr(CO)_3$ and (η^6-C_6H_5Cl)$Cr(CO)_3$ spectra compared to the (η^6-C_6H_6)$Cr(CO)_3$ spectrum is not caused by instrumental effects since the spectral resolutions are nearly identical for all the spectra, as was the pressure of the chemicals. We observe that the onset of detectable absorption of the (η^6-C_6H_6)$Cr(CO)_3$ spectrum occurs at lower energy than for the (η^6-C_6H_5Cl)$Cr(CO)_3$ and (η^6-$C_6H_5CH_3$)$Cr(CO)_3$ spectra and that the vibronic envelopes are different for the monosubstituted ACTs

(18) Beech, G. *Fortran IV in Chemistry*; Wiley: New York, 1975; p 127.
(19) Jørgensen, C. K. *Acta Chem. Scand.* **1954**, *8*, 1495.
(20) Klabuhn, B.; Spindler, D.; Goetz, H. *Spectrochim. Acta, Part A* **1973**, *29A*, 1283.

than for $(\eta^6\text{-}C_6H_6)Cr(CO)_3$. We also observe that there appears to be vibrational structure in the $(\eta^6\text{-}C_6H_5Cl)Cr(CO)_3$ and $(\eta^6\text{-}C_6H_5CH_3)Cr(CO)_3$ spectra that is not as distinct in the $(\eta^6\text{-}C_6H_6)Cr(CO)_3$ spectrum. The energy interval that characterizes the apparent vibrational structure is 621 cm^{-1} for $(\eta^6\text{-}C_6H_5Cl)Cr(CO)_3$, 598 cm^{-1} for $(\eta^6\text{-}C_6H_6)Cr(CO)_3$, and 647 cm^{-1} for $(\eta^6\text{-}C_6H_5CH_3)Cr(CO)_3$. This structure is probably less distinct than it would have otherwise been due to sequence congestion caused by combination bands that are hot with respect to lower frequency vibrations.

Discussion

Unlike the case of the closely related compound bis(benzene)chromium,[21] whose gas-phase spectroscopy we are pursuing, there are no recent ab initio calculations that attempt to provide the ordering of the $(\eta^6\text{-}C_6H_6)Cr(CO)_3$ excited electronic states. Hartree–Fock SCF and other calculations[22-31] have been performed mostly for the purpose of interpreting photoelectron spectra that only calculated the energies of those one-electron orbitals that are populated in the ground state. It is comforting to note that all the available calculations give essentially the same ordering, by symmetry type and energy, of the MOs that comprise the ACT ground-state configuration. The semiempirical treatment of McGlynn[27] gives an ordering for the lowest energy excited states: E, A_1, E, E, A_1, A_1, E. The calculation indicates that all seven of these states have energies below 38 000 cm^{-1}. No attempt was made to calculate states with energies above 45 000 cm^{-1}, and all have nonzero oscillator strength from the ground state. Most of the predicted oscillator strength involves two low-energy transitions, and in fact 95% of the sum of all the predicted oscillator strength involves only five transitions. However, the energies of these predicted transitions and our results are completely inconsistent with the deviations being large and bisignate. While we have no confidence in the accuracy of predicted absolute energies, it is conceivable that this calculation could correlate qualitative trends with some reliability and will be used as such. We would prefer to discuss all the experimental results in terms of band origins,[32] but because of the large overlaps between adjacent absorption features and the uncertainties in the widths of the Gaussians that modeled our spectra, we are unable to estimate the position of 0–0 bands from these low-resolution spectra.

The ordering of the excited states by energy and symmetry types predicted by McGlynn's calculation is actually consistent with our results, provided we assume that the excited E states are not split enough in energy to be resolved in our $(\eta^6\text{-}C_6H_5Cl)Cr(CO)_3$ and $(\eta^6\text{-}C_6H_5CH_3)Cr(CO)_3$ spectra. There is no question that a higher level calculation, perhaps an Xα–scattered-wave calculation that has given satisfactory predictions for bis(benzene)chromium, would help address the interpretation of our data. For our part, we are currently working toward providing higher resolution spectra that should reveal substituent-induced splittings and thus identify the E states. Since our resolution was on the order of a few hundred wavenumbers in the worst cases, we can state that the substituent-induced electronic splittings should be less than a few hundred wavenumbers. The splittings predicted by McGlynn are on the order of several hundred wavenumbers, so higher resolution, better than about 100 cm^{-1}, should be sufficient to observe the splittings. At this point, we cannot positively verify the correct ordering of excited states by energy and by symmetry type.

Comparisons of our spectra with solution-phase[33-39] results show that the gas-phase spectra consistently demonstrate a bathochromic shift when the solvent is nonpolar. We expect that this is at least partly a consequence of the elevated temperatures employed in our experiments. However, spectra recorded in polar solvents also reveal a bathochromic shift relative to those run in nonpolar solvents. The shift has been interpreted in terms of a solvent role in either providing relative destabilization of the excited states or stabilization of the ground states or both. On the basis of spectral shifts and intensity variations, nearly all the low-energy transitions have been previously assigned from solution-phase spectra as charge transfer in nature. McGlynn's calculation suggests that the 36 300-cm^{-1} transition is metal to CO, as is the 44 250-cm^{-1} transition, which also has some character of metal–arene to CO charge transfer. $Cr(CO)_6$ is known[33] to have strong absorptions at about 36 000 and 44 300 cm^{-1}, which are presumably analogous to these ACT transitions. Bis(benzene)chromium has only one transition[21] in this region, near 32 000 cm^{-1}, which may be related to our observations.

In the highest energy region we observe a feature at about 55 300 cm^{-1} for all the ACTs that could correspond to one-photon ionization to yield an ACT parent ion. This feature has no analogue in the spectrum of $Cr(CO)_6$, but there is a prominent feature in the spectrum of bis(benzene)chromium at 50 000 cm^{-1}. The exact energies of the maxima of this feature are consistently slightly lower than the reported ionization potentials[40-41] by electron impact. They do decrease in the order $(\eta^6\text{-}C_6H_5Cl)Cr(CO)_3 > (\eta^6\text{-}C_6H_6)Cr(CO)_3 > (\eta^6\text{-}C_6H_5CH_3)Cr(CO)_3$, as has also been observed in the electron-impact experiments. It is also possible that this feature is intra-arene in character, since the uncomplexed arenes[42] have a strong transition near this energy. It was precisely for this reason that we were particularly meticulous to ensure that our samples were pure and that neither photodecomposition nor thermal decomposition was occurring to any significant extent during our experiments. $(\eta^6\text{-}C_6H_6)Cr(CO)_3$ is known to manifest relaxation effects in photoelectron[22,23,43] and ESCA spectra[44] that imply the existence of excited states near 54 250 and 55 300 cm^{-1}, consistent with our observations. Higher spectral resolution, variable temperature, and scans extending to higher energy would greatly clarify this discussion.

We do have sufficient resolution to discern that there is one absorption feature that appears to shift substantially as the arene substituent is varied. There is a band predicted by McGlynn to occur at relatively high energy for the $(\eta^6\text{-}C_6H_5NH_2)Cr(CO)_3$ complex that he assigns to a predominantly arene substituent to

(21) Weber, J.; Geoffroy, M.; Toursot, A.; Penigault, E. *J. Am. Chem. Soc.* **1978**, *100*, 3995. See Table X and ref 3 and 25 of this reference for electronic spectra of bis(benzene)chromium.
(22) Guest, M. V.; Hillier, I. H.; Higginson, B. R.; Lloyd, D. R. *Mol. Phys.* **1975**, *29*, 113.
(23) Connor, J. A.; Derrick, L. M. R.; Hillier, I. H. *J. Chem. Soc., Faraday Trans. 2* **1974**, *70*, 941.
(24) Brown, D. A.; Rawlinson, R. M. *J. Chem. Soc. A* **1969**, 1534.
(25) Böhm, M. C. *J. Chem. Phys.* **1983**, *78*, 7044.
(26) Böhm, M. C. *J. Mol. Struct.* **1983**, *92*, 73.
(27) Carroll, D. G.; McGlynn, S. P. *Inorg. Chem.* **1968**, *7*, 1285.
(28) Elian, M.; Chen, M. M. L.; Mingos, M. P.; Hoffmann, R. *Inorg. Chem.* **1976**, *15*, 1148.
(29) Albright, T. A.; Hofmann, P.; Hoffmann, R. *J. Am. Chem. Soc.* **1977**, *99*, 7546.
(30) Saillard, J. Y.; Grandjean, D.; Choplin, F.; Kaufmann, G. *J. Mol. Struct.* **1974**, *23*, 363.
(31) Kok, R. A.; Hall, M. B. *J. Am. Chem. Soc.* **1985**, *107*, 2599.
(32) For a discussion of the relationship between calculated and experimental electronic transition energies, see: Trogler, W. C. *THEOCHEM* **1981**, *85*, 1.
(33) Baibich, I. M.; Butler, I. S. *Inorg. Chim. Acta* **1984**, *89*, 73.
(34) Mahaffy, C. A. L.; Rawlings, J. *Spectrosc. Lett.* **1984**, *17*, 765.
(35) Raznvaev, G. A.; Kuznetsov, V. A.; Egorochkin, A. N.; Klimov, A. A.; Artemov, A. N.; Sirotkin, N. I. *J. Organomet. Chem.* **1977**, *128*, 213.
(36) Trembovler, V. N.; Baranetskata, N. K.; Fok, N. V.; Zasuavskaya, G. B.; Yavorskii, B. M.; Setkina, V. N. *J. Organomet. Chem.* **1976**, *117*, 339.
(37) Lundquist, R. T.; Cais, M. *J. Org. Chem.* **1962**, *27*, 1167.
(38) Yamada, S.; Yamazaki, H.; Nishikawa, H.; Tsuchida, R. *Bull. Chem. Soc. Jpn.* **1960**, *33*, 481.
(39) Trembouler, V. N.; Yavorskii, B. M.; Setkina, V. N.; Baranetskaya, N. K.; Zaslavskaya, G. B.; Evdokimova, M. G. *Russ. J. Phys. Chem. (Engl. Transl.)* **1974**, *48*, 1231.
(40) Gilbert, J. R.; Leach, W. P.; Miller, J. R. *J. Organomet. Chem.* **1973**, *49*, 219.
(41) Herzberg, G. *Electronic Spectra of Polyatomic Molecules*; Van Nostrand Reinhold: New York, 1966; p 665.
(42) Muller, J. *J. Organomet. Chem.* **1969**, *18*, 321. Pignataro, S.; Lossing, F. P. *J. Organomet. Chem.* **1967**, *10*, 531.
(43) Gower, M.; Kane-Maguire, L. A. P.; Maier, J. P.; Sweigart, D. A. *J. Chem. Soc., Dalton Trans.* **1977**, 316.
(44) Pignataro, S.; Foffani, A.; Distefano, G. *Chem. Phys. Lett.* **1973**, *20*, 350.

CO charge-transfer transition. We note that the Gaussian analysis indicates a large hyperchromic and hypsochromic effect on the 49 500-cm^{-1} band of $(\eta^6\text{-}C_6H_6)Cr(CO)_3$ when a chlorine substituent is added. An opposite effect occurs when a methyl substituent is added. Although McGlynn's calculation dealt with an NH_2 substituent, it should be noted that his results may be a good indicator for the effect of a chlorine substituent as well. Experiments[35,45] and a calculation indicate that the effect of an arene substituent on the electronic structure of an ACT is correlated with the directing properties of the substituent in the reactivity pattern of the free substituted arene. Since an NH_2 group and a chlorine substituent are both ortho–para directing with regard to the free arene reactivity patterns, we might suspect that their effects on ACT electronic structure might be analogous in some other respects as well. We are inclined to tentatively assign the 49 000-cm^{-1} $(\eta^6\text{-}C_6H_5CH_3)Cr(CO)_3$, 49 500-$cm^{-1}$ $(\eta^6\text{-}C_6H_6)Cr(CO)_3$, and 52 800-$cm^{-1}$ $(\eta^6\text{-}C_6H_5Cl)Cr(CO)_3$ transitions to charge transfer from the metal–arene moiety to the CO's. This metal–arene-centered MO, which is depopulated in the transition, contains substantial contribution from the arene-substituent-centered atomic orbitals. Due to the reduced symmetry of the monosubstituted ACTs, one can construct MOs that only contain contributions from atomic orbitals localized on the substituent heteroatom and the other atoms contained in the C_s symmetry plane. The highly electronegative chlorine substituent could, relative to the toluene case, stabilize the (chlorobenzene)metal molecular orbital, which is depopulated in the charge-transfer transition. Assuming that the excited electronic state in this transition is of similar energies for the two ACTs, the shift in the absorption feature can be explained on the basis of a shift in ground electronic state energy. This argument is contingent upon knowing the correct assignment for this transition. In the absence of higher quality calculations and experiments, one can only speculate on possible assignments and explanations for the observed shift.

We now turn to a discussion of the higher resolution data. The repeating fine structure energy interval might correspond to a progression in a roughly 600-cm^{-1} vibration of either the ground or an excited electronic state. If the structure is in the excited electronic state, then some type of structural deformation occurs with the electronic transition. Taken at face value and based on the well-studied vibrational modes of the ground electronic state,[46] the magnitude of the observed vibrational spacing would seem to suggest a deformation involving either the metal to CO framework or the arene ring. The fact that many members of the possible progression are apparently visible suggests that the vibrational mode is totally symmetric. Among various possibilities it is equally plausible that all the observed members of the progression are even harmonics and that, in the case of $(\eta^6\text{-}C_6H_6)Cr(CO)_3$, the mode involves an A_2 vibration. In this case the vibrational frequency is about 300 cm^{-1} and the upper state quantum numbers are doubled. Although we certainly cannot resolve this assignment at this time, and there are many more possible assignments, we can note that our suggested assignment as a long vibrational progression is consistent with the well-known[11] photolability of the CO ligands in these molecules. Other workers have observed similar structure in $Cr(CO)_6$ at 10 K in an argon matrix, which they assigned to a M–C vibration. It is not certain that we can interpret our data similarly due to the higher temperature of our sample and due to the inherent structural differences of the molecules. For example, unlike that of $Cr(CO)_6$, the highest order symmetry axis contains none of the CO ligands. It seems remarkable that a molecule with 51 vibrational modes, many of them of relatively low energy, at elevated temperature, should not exhibit an absorption spectrum so inhomogeneously broadened as to be without any discernible fine structure at all. The fact that there is any discernible structure at all is very important. If the nonradiative lifetime of the upper states in these transitions were less than 10^{-13} s, we would not be able to observe 600-cm^{-1} fine structure due to homogeneous broadening of the upper states. So long as the source of the structure is not totally due to inhomogeneous broadening, 10^{-13} s represents a lower bound on the lifetime of the upper states.

The one-photon results present a view of ACT electronic structure that is consistent with our one-color multiphoton results.[6-8] The one-color multiphoton experiments were such that the incident radiation imparted between 27173 and 27250 cm^{-1} per photon. Note that, in the MPD/MPI experiment, absorption of photons, followed by dissociation and then absorption of additional photons by the dissociation products leading to their ionization, occurs within the duration of a single 20-ns laser pulse. We proposed that either radiationless transitions associated with intramolecular vibrational relaxation or photodissociation occurs after absorption of a single photon, which interrupts multiphoton excitation. The smoothness of the $(\eta^6\text{-}C_6H_5Cl)Cr(CO)_3$ and $(\eta^6\text{-}C_6H_5CH_3)Cr(CO)_3$ one-photon spectra compared to that of $(\eta^6\text{-}C_6H_6)Cr(CO)_3$ suggests that these molecules possess more low-frequency vibrations, which would lead to an increased radiationless transition rate compared to that of $(\eta^6\text{-}C_6H_6)Cr(CO)_3$. The possible progression that suggests a change in the metal to CO bonding and the lower limit on the dissociative lifetime inferred from that vibronic structure both leave the possibility of photodissociation on the time scale of multiphoton absorption plausible. We note that, in addition to the appreciable absorption strength observed at the single-photon level for the radiation used in our multiphoton experiments, there is a massive one-photon absorption at the two-photon level. Preliminary one-photon results near the three-photon level of our earlier MPD/MPI experiments indicate that there are no transitions as large as that observed at the two-photon level. Before we had obtained these one-photon spectra, we interpreted our multiphoton results by suggesting that some intact ACTs coherently absorb three photons before dissociating. We now suggest that the "coherent" pathway proposed[7] to be involved in our multiphoton experiments corresponds to either an initial two- or three-photon absorption by the ACTs. If the coherent step is only two photon, then the branching in the product state yields is probably based on a "dissociative ladder crossing" mechanism.[47] This is likely because thermodynamically an intact ACT could not absorb less than three photons ($\approx$27 173 cm^{-1}/photon) coherently and still dissociate to liberate the free chromium atoms in the excited states we observe. Since we know that many dynamic events in the MPD/MPI experiments proceed to completion on the time scale of the laser pulse, 20 ns, and the one-photon spectra suggest a unimolecular radiationless decay lifetime for isolated ACTs of at least 10^{-13} s, we have thus provided an upper and lower bound on the dynamic time scale for the MPD/MPI experiments. We believe this is very significant because if our estimates are correct, ACT photodissociation dynamics should occur on a time scale that is quite conveniently studied in real-time pump and probe experiments.

Conclusions

(Arene)chromium tricarbonyls have at least five excited electronic states with energies below 61 000 cm^{-1} that have allowed transitions from the ground state. Only one of these transitions is very sensitive to the addition of a substituent on the arene ring. Most of these transitions are charge transfer in character although intra-arene and one-photon ionization transitions are possible assignments for two of the transitions. There is a very strong transition at about 55 300 cm^{-1} for all the ACTs that may play a role in previously published multiphoton spectroscopy experiments. We demonstrate that the nonradiative lifetime of excited rovibronic states with energies between 25 000 and 32 000 cm^{-1} is greater than 10^{-13} s.

Acknowledgment. This research was supported by Syracuse University. We are indebted to C. G. Olson of Ames Laboratory for use of the beam line and electronics. Ames Laboratory is

(45) Jackson, W. R.; Jennings, W. B.; Rennison, S. C.; Spratt, R. *J. Chem. Soc. B* **1969**, 1214.
(46) Adams, D. M.; Squire, A. *J. Chem. Soc. A* **1970**, 814.
(47) Gedanken, A.; Robin, M. B.; Kuebler, N. A. *J. Phys. Chem.* **1982**, *86*, 4096.

operated for the U.S. Department of Energy by Iowa State University under Contract No. W-7405-ENG-82. We thank the staff of the Synchrotron Radiation Center of the University of Wisconsin—Madison for their excellent support. The Tantalus storage ring was supported by NSF Grant No. DMR 80-20164. We also made extensive use of the NIH Computational Resource at Syracuse University.

Registry No. $(\eta^6\text{-}C_6H_6)Cr(CO)_3$, 12082-08-5; $(\eta^6\text{-}C_6H_5Cl)Cr(CO)_3$, 12082-03-0; $(\eta^6\text{-}C_6H_5CH_3)Cr(CO)_3$, 12083-24-8.

Contribution from the National Biomedical ESR Center, Medical College of Wisconsin, Milwaukee, Wisconsin 53226, Department of Biophysics, Institute of Molecular Biology, Jagiellonian University, 31-120 Krakow, Poland, Faculdade de Filosofia Ciencias e Letras de Ribeirao Preto, Universidade de São Paulo, 01498 São Paulo, Brazil, and Department of Chemistry, University of Wisconsin–Milwaukee, Milwaukee, Wisconsin 53201

Assessment of the ESR Spectra of $CuKTSM_2$[1]

Marta Pasenkiewicz-Gierula,[†‡] William E. Antholine,*[†] Witold K. Subczynski,[†‡] Oswaldo Baffa,[†§] James S. Hyde,[†] and David H. Petering[∥]

Received March 3, 1987

The nitrogen superhyperfine structure in the ESR spectrum for $CuKTSM_2$ in light paraffin oil is particularly well resolved in the rigid-limit and fast-tumbling regions. This oil is an excellent solvent because its viscosity, to a first approximation, is similar to the viscosity in cell membranes, the dielectric properties of paraffin oil are suitable for the solvation of $CuKTSM_2$, and the acyl chains help maintain $CuKTSM_2$ monomers throughout a wide range of concentrations and temperatures. Computer curve fitting, including Monte Carlo and damped-least-squares methods, is used to obtain ESR parameters. The refinement of the ESR parameters based on the determination of the goodness of fit is a new approach to ESR analysis. Near-rigid-limit spectra obtained by increasing the temperature from −40 to about +10 °C have fewer resolved lines in the perpendicular region and no resolved superhyperfine lines in the low-field portion of the parallel region. Use is made of only these lines in the perpendicular region to determine the number of nitrogen donor atoms from the ESR spectrum.

Introduction

In the early 1960s French and Freelander, who screened hundreds of compounds, found that 3-ethoxy-2-oxo-butyraldehyde bis(thiosemicarbazone), H_2KTS, is one of four thiosemicarbazones that have significant activity against sarcoma 180 in mice.[2] Then Petering and co-workers[3,4] proved that H_2KTS is active as the copper complex, CuKTS (Figure 1). High toxicity for H_2KTS was reported following a phase I clinical study,[5] but many of the toxic symptoms can be attributed to interference with copper metabolism.[4] Subequently, Petering and co-workers studied the chemical properties of CuKTS and the interactions that occur upon addition to Ehrlich ascites tumor cells.[6] It was concluded that ligand substitution or addition will be thermodynamically or kinetically unfavorable in vivo, but CuKTS is slowly reduced and dissociated by thiols, primarily glutathione, in cells. For derivatives of CuKTS, a linear free energy correlation between the relative pseudo-first-order rate constants of reaction of these complexes with cells as a function of their reduction potentials indicated that complexes with sufficient reactivity toward sulfhydryl groups are also active against cells.[6] Recent studies show that some copper is transferred to metallothionein.[7]

Previous ESR studies on the interaction of CuKTS derivatives with Ehrlich cells established that CuKTS is rapidly reduced whereas $CuKTSM_2$ (Figure 1) is stable in cells over several hours.[8,9] ESR studies show that the mobility of $CuKTSM_2$ in cells at room temperature is so slow that its spectrum indicates immobilization.[9] As the concentration of $CuKTSM_2$ in Ehrlich cells increases, an additional spectrum characteristic of fast motion is superimposed upon the slow-motion spectrum.[9,10] $CuKTSM_2$ is cytotoxic toward Ehrlich cells at a concentration for which both immobile and mobile $CuKTSM_2$ spectra are recorded. Whether either form or both of these forms are related to cytotoxicity has not yet been determined. It is known that the immobile form dominates in spectra from artificial lipid bilayer preparations above and below the main phase transition temperature.[11] ESR spectra in oriented artificial membranes are consistent with a hypothesis in which $CuKTSM_2$ is well oriented with the plane of the complex perpendicular to the bilayer surface and parallel to the acyl chains.[11] Translational diffusion of $CuKTSM_2$ in a bilayer depends on phospholipid alkyl chainlengths, unsaturation, and the presence of cholesterol.[11,12]

In this article we present ESR spectra of $CuKTSM_2$ in paraffin oil at several different temperatures. Light paraffin oil is a particularly suitable solvent because the motion of $CuKTSM_2$ in paraffin oil may resemble, to a rough first approximation, the motion of $CuKTSM_2$ in artificial bilayers and cell membranes.[9] The oil is a mixture of saturated hydrocarbon chains of various lengths. Translational diffusion of $CuKTSM_2$ in paraffin oil is slow, and collisions between $CuKTSM_2$ molecules (Heisenberg exchange) are infrequent.[13] Rotational diffusion is probably faster because the average size of the solvent molecule is similar to the size of $CuKTSM_2$ and because the possibility of microscopic

* To whom correspondence should be addressed.
† Medical College of Wisconsin.
‡ Jagiellonian University.
§ Universidade de São Paulo.
∥ University of Wisconsin—Milwaukee.

(1) This work was supported by NIH grants GM35472 and RR01008 and the University of Wisconsin—Milwaukee. O.B. was supported by the John Simon Guggenheim Foundation and CAPES.
(2) French, F. A.; Freedlander, R. L. *Can. Res.* **1960**, *21*, 505–538.
(3) Petering, H. G.; Van Giessen, G. J. In *The Biochemistry of Copper*; Peisach, J., Aisen, P., Blumberg, W., Eds.; Academic: New York, 1966; pp 197–210.
(4) Petering, D. H.; Petering, H. G. In *Handbook of Experimental Pharmacology*; Sartorelli, A. C., Johns, D. G., Eds.; Springer-Verlag: New York, 1975, Vol. 30, Part II, p 841.
(5) Regelson, W.; Holland, J. F.; Talley, R. W. *Cancer Chemother. Rep.* **1967**, *51*, 171–177.
(6) Petering, D. H.; Antholine, W. E.; Saryan, L. A. In *Metal Complexes as Antitumor Agents in Anticancer and Interferon Agents*; Ottenbrite, R. M., Butler, G. B., Eds.; Marcel Dekker: New York, 1984; pp 203–246.
(7) Kraker, A.; Krezoski, S.; Schneider, J.; Minkel, D.; Petering, D. H. *J. Biol. Chem.* **1985**, *260*, 13710–13718.
(8) Minkel, D. T.; Petering, D. H. *Cancer Res.* **1978**, *38*, 117–123.
(9) Antholine, W. E.; Basosi, R.; Hyde, J. S.; Lyman, S.; Petering, D. H. *Inorg. Chem.* **1984**, *23*, 3543–3548.
(10) Antholine, W. E.; Subczynski, W. K.; Hyde, J. S.; Petering, D. H. In *Biology of Copper Complexes*; Sorenson, J. R. J., Ed.; Humana: Clifton, NJ, in press.
(11) Subczynski, W. K.; Antholine, W. E.; Hyde, J. S.; Petering, D. H. *J. Am. Chem. Soc.* **1987**, *109*, 46–52.
(12) Subczynski, W. K.; Antholine, W. E.; Hyde, J. S.; Kusumi, A., submitted for publication in *Inorg. Chem.*
(13) Subczynski, W. K.; Hyde, J. S. *Biophys. J.* **1984**, *45*, 743–748.

0020-1669/87/1326-3945$01.50/0 © 1987 American Chemical Society